IEEE Access
Multidisciplinary | Rapid Review | Open Access Journal

Received May 14, 2020, accepted May 30, 2020, date of publication June 15, 2020, date of current version June 29, 2020.

Digital Object Identifier 10.1109/ACCESS.2020.3002545

Automatic Early Broken-Rotor-Bar Detection and Classification Using Otsu Segmentation

MISAEL LOPEZ-RAMIREZ[1], (Member, IEEE), LUIS M. LEDESMA-CARRILLO[1], (Member, IEEE), FRANCISCO M. GARCIA-GUEVARA[1], JORGE MUNOZ-MINJARES[2], EDUARDO CABAL-YEPEZ[1], (Member, IEEE), AND FRANCISCO J. VILLALOBOS-PINA[3], (Member, IEEE)

[1]Engineering Division, Multidisciplinary Studies Department, University of Guanajuato, Guanajuato 38944, Mexico
[2]Electronics Engineering Department, Autonomous University of Zacatecas at Jalpa, Jalpa 99601, Mexico
[3]National Institute of Technology of Mexico/Aguascalientes Institute of Technology, Aguascalientes 20256, Mexico

Corresponding author: Luis M. Ledesma-Carrillo (l.m.ledesmacarrollo@gmail.com)

This work was supported in part by Direccion de Apoyo a la Investigacion y al Posgrado (DAIP), University of Guanajuato, Through the Program Funding for Faculty Members, 2020.

ABSTRACT Induction motors (IM) are susceptible to mechanical failures with severe consequences for production lines; hence, detection and classification of IM faults have been of great interest for researchers in last years. Broken rotor bars (BRB) are one of the most difficult faults to detect, since this fault does not give any indication of deterioration increasing significantly the production costs; hence, it is quite important to detect them in early states. Several methodologies have been proposed to extract information about the motor condition relying on motor-current-signature analysis (MCSA); however, they usually require high-computational-complexity algorithms to reach trustworthy result. In this work, a novel methodology for early detection and classification of BRB faults in IM is proposed. This methodology consists of obtaining two spectrograms using fixed-width windows, which are segmented through Otsu algorithm to visualize the time evolution of fault frequencies. The fault severity classification is performed through Kurtosis computation from non-stationary components. Obtained results from real experimentation validate the proposed-method high efficiency, reaching an overall 100% accuracy on detecting and classifying half, one, two BRBs, and healthy condition.

INDEX TERMS Early broken-rotor-bar detection, induction motor, kurtosis, Otsu segmentation, time-frequency distribution.

I. INTRODUCTION

Induction motors (IM) are very important in the modern industry because they are the main source of mechanical power. They have advantages such as its low price, stiffness, and reliability. However, this type of electric machines is susceptible to mechanical failures, which can lead to interruptions in production lines, resulting in serious consequences, raising manufacturing costs and decreasing quality of products. Therefore, detection and classification of IM faults have gained great attention from researchers in recent years [1]–[3]. Among the most difficult faults to detect are Broken Rotor Bars (BRB). This is a silent failure that allows operating the motor without giving any indication of deterioration, increasing the harmonic distortion and causing a significant increase in production costs [3]. Hence, early detection and classification of BRB is desirable, since operating under this condition can be catastrophic for IM [4]–[7].

The most used method for detecting BRB faults is the motor current signature analysis (MCSA), which usually is based on non-invasive electric-current measurement [8]–[11]. Therefore, several methodologies have been proposed to extract information about the motor condition relying on MCSA. One common technique for IM fault detection is the Fast Fourier Transform (FFT) [12], [13], and its variations; for instance, the short-time Fourier transform (STFT) [14], the Gabor transform (GT) [15] and the method of selection of amplitudes of frequencies ratio 50 second frequency coefficient (MSAF-RATIO-50-SFC) [16], [17], which are suitable for information extraction from non-stationary signals. However, the windowing length has a direct effect on the time and frequency resolution.

The associate editor coordinating the review of this manuscript and approving it for publication was Jiafeng Xie.

Short-length windows provide high resolution in time with low resolution in frequency; otherwise, long-length windows provide the opposite effect.

On another hand, the quadratic time-frequency distribution (QTFD) has been used because of its independence from the type or size of the window and its inherent suitability for analyzing non-stationary signals [12]; hence, several QTFD-based methods have been implemented for classifying IM faults [11], [12]. In [11], a performance comparison between the GT and the Wigner-Ville distribution with Choi-Williams kernel is presented to detect BRB in IM. The Choi-Williams kernel is used for suppressing cross-terms on QTFD, to get better time and frequency resolution, compared to the GT. In [12], a technique for detecting and diagnosing rolling bearing faults based on high-order synchrosqueezing transform (FSSTH) and detrended fluctuation analysis (DFA) is presented. The vibration signal is decomposed using FSSTH into an ensemble of oscillatory components; then, the number of intrinsic mode functions is determined through an DFA-based empirical equation. Fault characteristic frequencies are identified using a time-frequency representation. Other techniques have been used for BRB detection too, which just provide high-frequency resolution. For instance, a multiple signal classification (MUSIC) for order selection during BRB detection in IM is presented in [5], where authors introduce a feature extraction from frequency spectra components using an automatic parameter selection for an optimal spectrum representation. In [18], bearing and BRB faults are detected using high-resolution spectral analysis using MCSA by separating frequency components close to the fundamental one. The fault severity is estimated from the amplitudes computed from least squares estimator. On the other hand, many artificial intelligence methods such as artificial neural networks (ANN), fuzzy logic (FL) and support vector machines (SVM) have been employed to improve the effectiveness of fault detection and classification in IM [19]. Although, many of the above-mentioned techniques provide high efficiency for BRB detection and classification, the major drawback in most of them is their high computational complexity. Hence, new methodologies based on traditional techniques such as the STFT are still being used [20], [21]. For instance, a methodology based on FFT is presented in [20] to detect BRB conditions. The approach consists of two windows moving along the analyzed current signal for subtracting the spectral information from both windows to get the non-stationary frequencies. In [21], broken rotor bars are detected considering that the fault-related harmonics will have oscillating amplitudes due to the speed ripple effect. A time-frequency transformation is used where fault-related frequencies are treated as periodical signals over time and fast Fourier transform is used for assessing spectral contents leading to the discrimination of subcomponents related to the fault and the estimation of their amplitudes. However, nearly none of the above are able to detect half BRB. Hence, reliable identification of half BRB is still open field under investigation as they are really difficult to detect [22]–[27].

In this paper a novel methodology for early detection and classification of BRB faults in IM is proposed. This methodology consists of using multiple-STFT with two different fixed-width windows (Gaussian, Kaiser). The obtained spectrograms using each window are subtracted to highlight the differences between them and obtain a reliable threshold. The non-stationary frequencies are segmented using Otsu algorithm to visualize the evolution in time of the fault frequency. Finally, Kurtosis is obtained from these non-stationary components as a classification parameter. In addition, the three-sigma rule is used for demonstrating the proposed method effectiveness for early detection of BRB in IM. Obtained results using the proposed methodology on acquired data from real experimentation validate its high efficiency, achieving an overall accuracy of 100% on discriminating among one, two BRBs, and healthy condition, and even detecting half broken bar, which nearly none of the methods in reviewed literature achieve.

II. THEORETICAL BACKGROUND

A. BROKEN ROTOR BARS

Induction Motor Broken-Rotor-Bars (BRB) detection in steady-state can be performed by the observation of the characteristic broken-bar harmonic components (f_{BRB}) in stator line-current [5], [7], [28]. These frequencies are given in (1),

$$f_{BRB} = f_C\,(1 \pm 2s) \tag{1}$$

where f_C is the fundamental frequency of the current supply, and s is the dimensionless motor slip, and it is calculated as:

$$s = \frac{n_1 - n}{n_1} \tag{2}$$

where n_1 and n are the synchronous and the rotor speed, respectively. On the other hand, the rotor speed changes during the start-up transient, which causes the BRB characteristic frequency changes over time too, until reaching the steady state. The theoretical harmonic-component trajectories show a linear evolution of the slip, and they are shown in Fig. 1. These well-known Lower and Upper Sideband Harmonic components (LSH and USH, respectively) are depicted in this figure [28].

B. SHORT-TIME FOURIER TRANSFORM AND SPECTROGRAM

To obtain the localized spectrum of a signal $x(t)$ at time $t = \tau$, the first step is to multiply $x(t)$ by the window $w(t)$, centered on the time $t = \tau$, obtaining

$$x_w(\tau, t) = x(t)\, w(t - \tau)\,. \tag{3}$$

Fourier Transform (FT) is applied to the windowed function obtained from (3) to produce (4).

$$F\{x_w(\tau, t)\} = F_x^w(\tau, \omega) = \underset{t \to \omega}{F}\{x(t)\, w(t - \tau)\} \tag{4}$$

where $F_x^w(\tau, \omega)$ is called the short-time Fourier transform (STFT), which shows the time evolution of the frequency

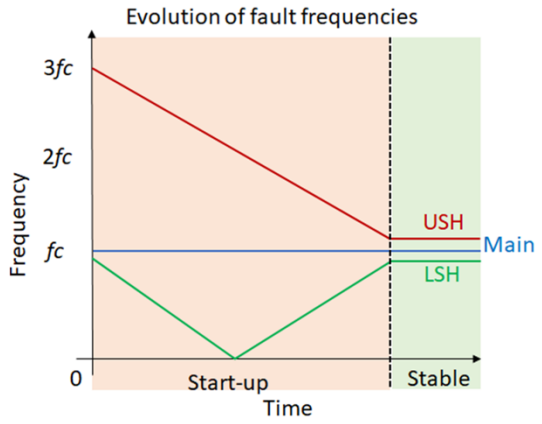

FIGURE 1. Theoretical trajectories of characteristic BRB harmonic components during the IM start-up transient.

components ω in $x(t)$, where $\omega = 2\pi f$. The squared magnitude of the STFT, denoted by $S_x^w(\tau, \omega)$, is called the spectrogram [29]:

$$S_x^w(\tau,\omega) = \left|F_x^w(\tau,\omega)\right|^2 \tag{5}$$

$$= \left|\underset{t\to\omega}{F}\{x(t)\,w(t-\tau)\}\right|^2 \tag{6}$$

$$= \left|\int_{-\infty}^{\infty} x(t)\,w(t-\tau)\,e^{-j\omega t}dt\right|^2 \tag{7}$$

In this paper $w(t)$ takes the Gaussian and Kaiser windows, $w_g(t)$ and $w_k(t)$ respectively. The coefficients of discrete Gaussian window $w_g(n)$ are computed from the following equation

$$w_g(n) = \mathrm{e}^{-\left(\alpha\frac{n-(N/2)}{2(N+1)}\right)^2} \tag{8}$$

where N is the window length and α is inversely proportional to the standard deviation [30]; whereas the discrete window $w_k(n)$ is defined as:

$$w_k(n) = \begin{cases} \dfrac{I_0\left[\pi\alpha\sqrt{1-\left(2n/N\right)^2}\right]}{I_0[\pi\alpha]} & |n| \le N/2 \\ 0 & 0 > N/2 \end{cases} \tag{9}$$

where I_0 is the zeroth-order modified Bessel function of the first kind, and α is a non-negative real number that determines the shape of the window [31], [32].

C. OTSU THRESHOLD

Otsu algorithm is a nonparametric and unsupervised method for computing an automatic threshold in an image. In this work, it is adapted to be able to work with a TFD treating it as a gray-scale level image. The histogram is normalized and regarded as a probability distribution P_i [33], [34].

$$P_i = \frac{n_i}{M}, \quad P_i \ge 0, \quad \sum_{i=1}^{L} P_i = 1 \tag{10}$$

where L is the total number of gray-levels, M is the number of pixels or data in TFD, and n_i is the repetition rate of pixels with an energy level i in the TFD. Then the pixels are split into two classes C_0 and C_1 (background and objects or vice versa) by a threshold at level k. Therefore, each class occurrence probability P_r and its corresponding mean level μ_r are given by:

$$z_0 = Pr(C_0) = \sum_{i=1}^{k} P_i = z(k) \tag{11}$$

$$z_1 = Pr(C_1) = \sum_{i=k+1}^{L} P_i = 1 - z(k) \tag{12}$$

$$\mu_0 = \sum_{i=1}^{k} iPr(i|C_0) = \frac{\mu(k)}{z(k)} \tag{13}$$

$$\mu_1 = \sum_{i=k+1}^{L} iPr(i|C_1) = \frac{\mu_T - \mu(k)}{1 - z(k)} \tag{14}$$

where $\mu(k)$ indicates the arithmetic mean for each level k, and μ_T is the total mean for all L levels, which are given by:

$$\mu(k) = \sum_{i=1}^{k} iP_i \tag{15}$$

$$\mu_T = \sum_{i=1}^{L} iP_i \tag{16}$$

Each class variance is given by:

$$\sigma_0^2 = \sum_{i=1}^{k} (1-\mu_0)^2 \frac{P_i}{z_0} \tag{17}$$

$$\sigma_1^2 = \sum_{i=k+1}^{L} (1-\mu_1)^2 \frac{P_i}{z_1} \tag{18}$$

The discriminating factor η to separate between two classes (C_0 and C_1) is given as:

$$\eta = \frac{\sigma_B^2}{\sigma_T^2} \tag{19}$$

where

$$\sigma_B^2 = z_0 z_1 (\mu_1 - \mu_0)^2 \tag{20}$$

$$\sigma_T^2 = \sum_{i=1}^{L} (i-\mu_T)^2 P_i \tag{21}$$

The optimal threshold k^* that maximizes η or equivalently maximizes σ_B^2 is give by:

$$\sigma_B^2(k^*) = \max_{1\le k\le L}\left(\sigma_B^2(k)\right) \tag{22}$$

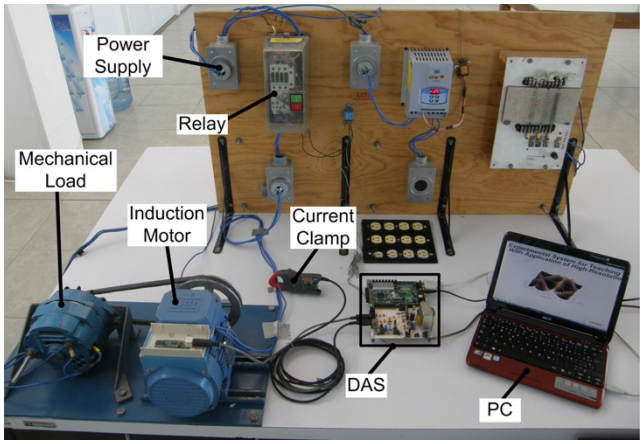

FIGURE 2. Test bench for experimentation.

D. KURTOSIS

Kurtosis is used to measure whether the data is peaked or flat relative to a normal distribution. Data sets with high kurtosis have a distinct peak near to the mean. They decline rapidly and have heavy tails. In contrast to those sets with low kurtosis, which have a flat top near the mean. A uniform distribution would be the extreme case [35]. The kurtosis K of a random event $Y = \{y_1, y_2, \ldots, y_n\}$ is defined as:

$$K = \frac{\sum_{i=1}^{n} (y_i - \mu)^4}{\sigma^4} \tag{23}$$

where y_i is equivalent to the spectrogram P_i.

III. EXPERIMENTAL SETUP

The proposed methodology was validated experimentally through the test bench shown in Fig. 2. It consists of 1 HP three-phase induction motor, model WEG 00136APE48T, which is fed directly from the power line, and has the following features:

a) 2 poles.
b) Rotor with 28 bars.
c) Power supply of 220 V/AC at 60 Hz.

The proposed method was tested using a healthy motor, a motor with half broken rotor bar, a motor with one broken rotor bar and a motor with two adjacent broken rotor bars.

The broken-rotor-bar conditions were produced artificially by drilling holes with 7.938 mm diameter on each bar without harming the shaft. Fig. 3 shows the rotors with broken bars used during experimentation. The mechanical load condition was established by connecting an ordinary alternator, which represents a quarter of the nominal load for the induction motor. The powerline-supplied current signal is acquired using an AC clamp model i200s from Fluke. The data acquisition system (DAS) consists of an analog-to-digital converter (ADS7809) with 16-bit resolution. The DAS uses a sampling frequency $f_s = 1.5$ kHz, obtaining 4,096 samples in 2.7 seconds during the motor start-up transient.

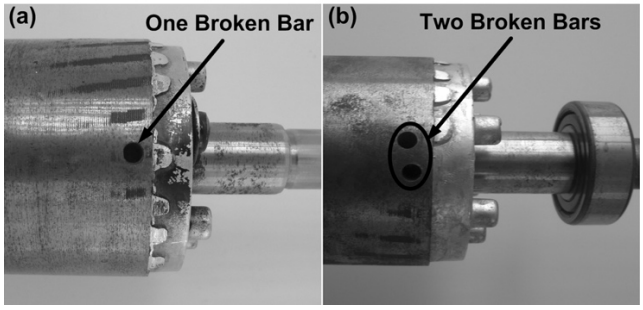

FIGURE 3. (a) One Broken Rotor Bar (1BRB), (b) Two Broken Rotor Bar (2BRB).

IV. PROPOSED METHODOLOGY

The proposed methodology is depicted in Fig. 4. It consists of the current-signal acquisition from one phase of the power supply during the IM start-up transient. The obtained discrete signal is resampled from 1.5 kHz to 256 Hz, reducing the number of analyzed data and processing time. Two STFTs are computed applying a Gaussian and a Kaiser window to each of them, respectively, both with a $\sigma = 2.5$, producing a trade-off resolution between time and frequency, with a large contribution of spurious frequencies. Therefore, spurious frequencies are eliminated by subtraction and segmentation, keeping the distinctive BRB fault frequency components. Otsu algorithm is used for defining the optimal threshold to eliminate spurious frequencies, segmenting the spectrogram calculated using the Kaiser window. Kurtosis is calculated from the segmented-TFD histogram as a discriminant parameter among the healthy case, and the faulty cases with Half BRB, One BRB, and Two BRB.

V. DETECTION AND CLASSIFICATION

The effectiveness of the proposed methodology on detecting and classifying BRB in an IM was validated by obtaining 20 sets of the discretized electric current signal supplied to the IM under each motor condition; each set is composed of 700 samples. Fig. 5 shows the different stages of the proposed methodology, where, the sampled period was 2.73 s of the start-up transient current signal. The time evolution of the related harmonics for each motor condition (HBRB, 1BRB, and 2BRB) during the start-up is identified as:

1.- Lower Sideband Harmonic (LSH).
2.- Upper Sideband Harmonic (USH)).

The STFT spectrograms with Gaussian and Kaiser windowing, along with Otsu segmentation provide an outstanding representation of the BRB characteristic frequency evolution in time, for the 3 faulty cases treated in this work, during the start-up transient. However, there is a difficulty on discriminating among them; therefore, it is necessary to implement an automatic sorting method for improving the classification into each faulty condition (HBRB, 1BRB and 2BRB). Hence, a simple and efficient classifier based on normal distribution is used in this work, demonstrating a high

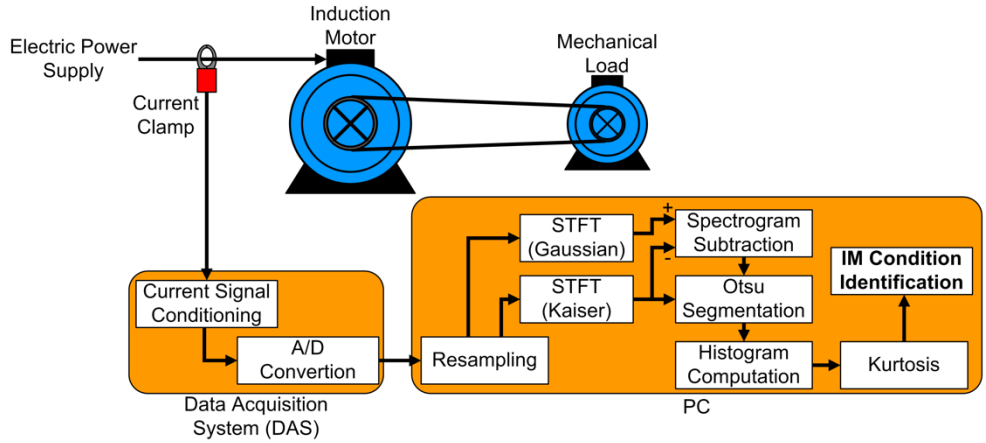

FIGURE 4. Proposed methodology for the detection and classification of early BRB in IMs.

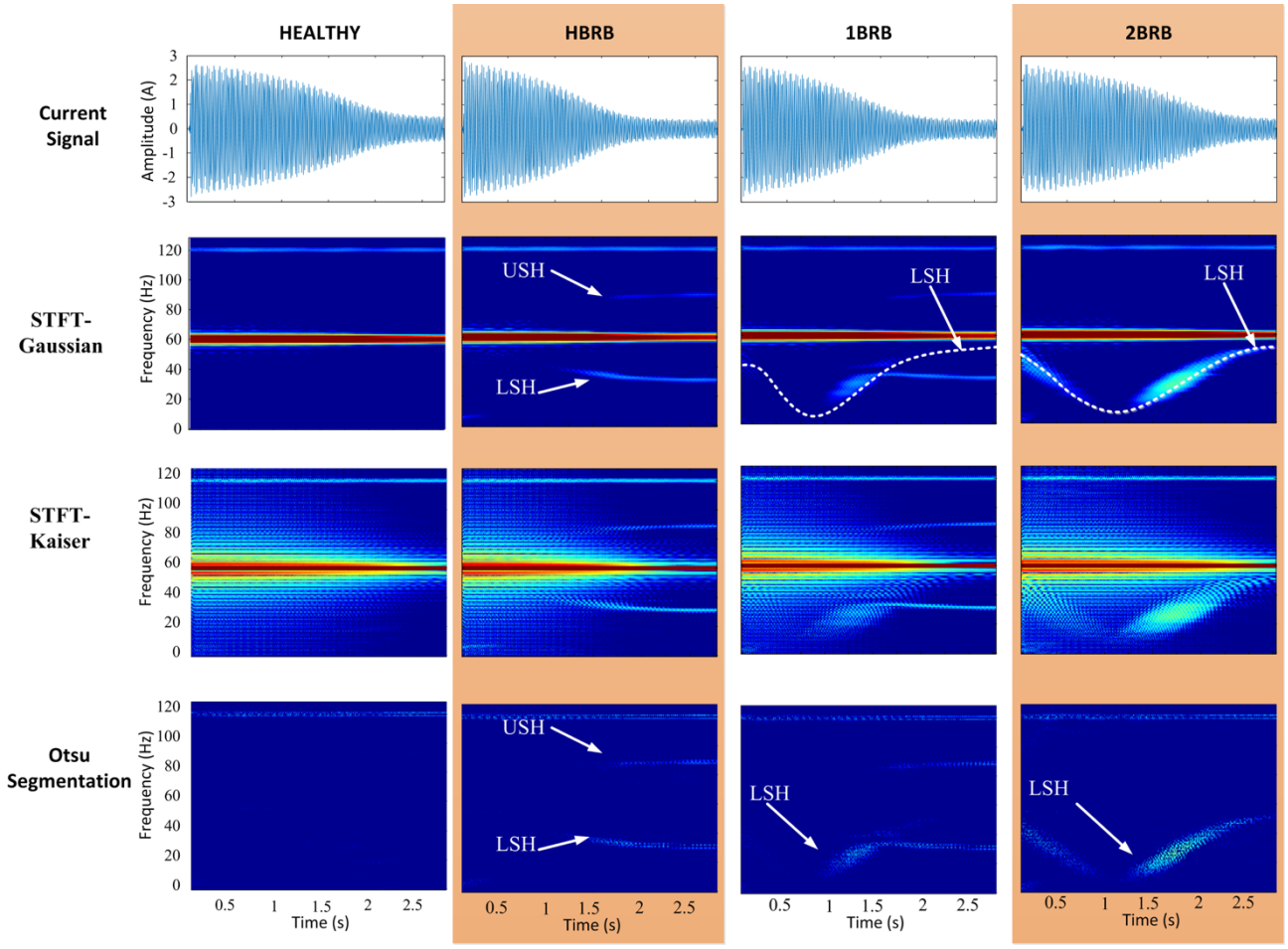

FIGURE 5. Proposed methodology stages during IM operational condition detection and classification.

performance of the proposed methodology for detecting and classifying BRB.

A. FAULT EXTRACTION

Kurtosis parameter is used as a discriminant parameter for classification of the fault severity. Its computation starts by taking the segmented time-frequency representation shown in the bottom row of Fig. 5. This TFD is obtained as a color image, so it is necessary to convert it to its grayscale representation in order to obtain the corresponding 256-level intensity histogram. From the obtained histogram, the kurtosis is estimated and used as a discriminant parameter for

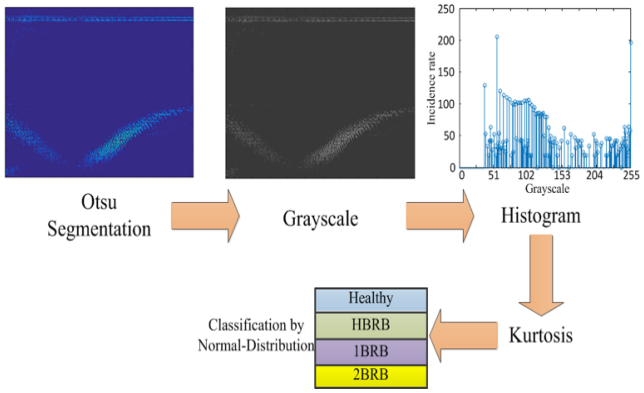

FIGURE 6. Condition classification from the segmented TFD and its corresponding Kurtosis computation.

TABLE 1. Statistical parameters of kurtosis for each treated condition.

	μ	σ
Healthy	253.86	0.0187
HBRB	253.59	0.0301
1BRB	253.06	0.0663
2BRB	252.65	0.0632

severity classification of the treated faults. The procedure is depicted in Fig. 6.

B. CLASSIFICATION

The kurtosis gives a numerical value to identify the motor condition into four different classes [3]: 1) Healthy, 2) Half-Broken Rotor Bar (HBRB), 3) One-Broken Rotor Bar (1BRB), and 4) Two-Broken Rotor Bar. The normal distribution, given in (24), of the kurtosis value is used in this work as classification parameter to identify the induction-motor condition.

$$PDF(\mathrm{K}:\mu,\sigma^2)=\frac{1}{\sqrt{2\pi\sigma^2}}\exp\left(-\frac{(K-\mu)^2}{2\sigma^2}\right) \quad (24)$$

In (24), μ is the mean, σ is the standard deviation and σ^2 is the variance. The mean and standard deviation are computed according to (15) and (17), respectively, applying Otsu segmentation on the obtained histogram from 20 trials for each treated motor condition. Table 1 shows the statistical parameters for the probability density distribution that defines the membership and rejection regions of each treated case through the empirical three-sigma (3σ) rule, which ensures a 99.7% effectiveness during the motor operation-state classification. Hence, the three-sigma limits are used as optimum thresholds for performing the automatic detection and classification of each condition (Healthy, HBRB, 1BRB or 2BRB). The probability density for each treated case is shown in Fig. 7.

C. EFFECTIVENESS VALIDATION

The accuracy of the proposed methodology for detecting and classifying an induction motor operational condition is

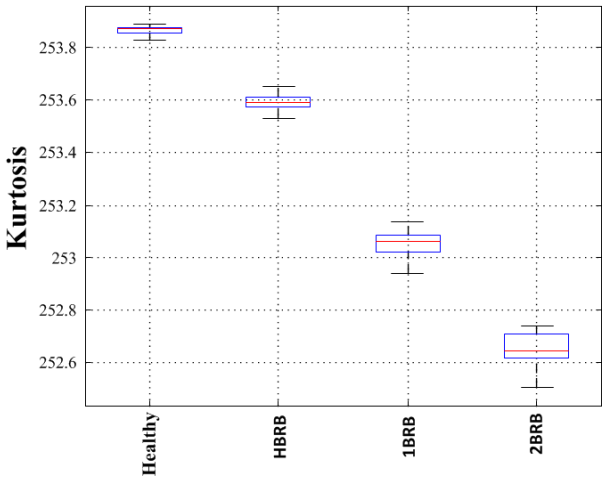

FIGURE 7. Box plot for BRB severity classification in IM.

TABLE 2. Proposed-methodology classification effectiveness.

	Health	HBRB	1BRB	2BRB	Accuracy(%).
Healthy	20	0	0	0	100
HBRB	0	20	0	0	100
1BRB	0	0	20	0	100
2BRB	0	0	0	20	100
Overall success rate					**100**

assessed in terms of its four different outcome metrics as:

$$\text{Accuracy}(\%)=\frac{TP+TN}{TP+TN+FP+FN}\times 100\% \quad (25)$$

where *TP*, *TN*, *FP* and *FN*, are the true positive, true negative, false positive, and false negative rates, respectively. These values are given as the occurrence of the positive (correctly classified) and negative (incorrectly identified) outcomes during an operational condition determination [35]. Table 2 shows the confusion matrix containing information about actual and estimated classification for 20 new trials on every induction-motor operational condition. Obtained results validate the high effectiveness of the proposed methodology with an overall accuracy of 100%.

VI. DISCUSSION

Table 3 shows a qualitative comparison of recent applied techniques reported in the literature, against the introduced in this work, for early detection and classification of BRB in IM, regarding percentage load torque, processing time and classification effectiveness. Taking into account this comparison, the proposed methodology shows high accuracy in the detection and classification of broken rotor bars, reaching at least the same sensitivity and effectiveness than others approaches; although, it has been extensively proven that the higher the fault severity and/or the mechanical load, the easier the BRB detection [26], [27], [36]–[41]. Furthermore, it is desirable to have a visual representation of the fault-frequency evolution in time, to corroborate the diagnosis of the induction motor operational condition. Hence, it is noteworthy that the proposed methodology classifies the faulty condition during the start-up transient under only 25% of

TABLE 3. Comparison chart of the proposed methodology against previous approaches.

Time-frequency Methodology	Applied Techniques	Load Torque (%)	Processing Time	Analyzed State	Display of Fault Frequencies	Effectiveness (%)			
						Healthy	HBRB	1BRB	2BRB
Rivera *et al* 2018 [20]	1.- Tooth-FFT 2.- Pearson correlation	50	Not Reported	Transient	Yes	90	100	100	100
Wang *et al* 2019 [36]	1.- Cyclic modulation Spectrum 2.- Window Functions	60 80	26.17s	Steady	Not	100	-	100	100
Soleimani *et al* 2019 [37]	1.- Air-gap rotational magnetic field 2.-logic gates	25 50 100	17.5ms	Steady	Not	-	-	-	-
Zhao et al 2019 [38]	1.- Multivariate Relevance Vector Machine 2.- Multiple Gaussians 3.-Principal component Analysis	75	Not Reported	Steady	Not	100	-	100	80
Jiang *et al* 2018 [39]	1.-Broad Learning Theory 2.-EMD 3.-statistical Features	75	Not Reported	Steady	Not	-	-	92.94	-
Contreras *et al* 2019 [40]	1.- Quaternion Signal Analysis 2.-Classification Bayesian	25	275.6ms	Steady	Not	100	-	100	-
Glowacz A. 2018 [41] Method 1.	1.- SMOFS-32-MULTIEXPANDED-2-GROUPS 2.- Neural Network	-	Not Reported	Steady	Not	100	-	100	100
Glowacz A. 2018 [41] Method 2.	1.- SMOFS-32-MULTIEXPANDED-1-GROUPS 2.- Nearest Neighbour	-	Not Reported	Steady	Not	100	-	100	93
Proposed	**1.- Multi-STFT 3.- Otsu Segmentation 2.-Normal-distribution**	**25**	**20.7ms**	**Transient**	**Yes**	**100**	**100**	**100**	**100**

its nominal mechanical load providing a graphical representation of the fault-frequency evolution in time. Finally, the effectiveness of the proposed method shows a 100% accuracy during the classification of all treated cases, including HBRB, which is one of the most difficult faults to detect; thus, from all described above, it is demonstrated that the proposed methodology is a reliable, efficient and practical technique for broken-rotor-bar detection and classification.

VII. CONCLUSION

Induction motors are very important in the modern industry; hence, failures in these electric machines generate serious consequences for industry. Broken rotor bars are among the faults more difficult to detect; thus, early detection and classification of these faults have gained a lot of interest by the scientific community. Several approaches, based on motor current signature analysis, have been proposed for extracting information about the induction motor condition; however, their major drawback is the high computational complexity for classification. In this work a novel methodology for early detection and classification of BRB in IM is proposed using STFT with Gaussian and Kaiser windowing and Otsu algorithm. Quantitative and qualitative analyzes against recent applied techniques reported in the literature demonstrate the high effectiveness of the proposed method for detecting and classifying the motor condition as: Healthy (HLT), Half-Broken Rotor Bar (HBRB), One-Broken Rotor Bar (1BRB) or Tow-Broken Rotor Bar (2BRB) with a 100% accuracy, providing a reliable, efficient and practical technique for early broken-rotor-bar detection and classification with low computational cost and a graphical representation of the fault-frequency evolution in time. Future work might include studying different types of faults and trying other time-frequency representations to perform the analysis under different operational conditions including power supply through a variable speed drive.

REFERENCES

[1] M. Z. Ali, M. N. S. K. Shabbir, X. Liang, Y. Zhang, and T. Hu, "Machine learning-based fault diagnosis for single- and multi-faults in induction motors using measured stator currents and vibration signals," *IEEE Trans. Ind. Appl.*, vol. 55, no. 3, pp. 2378–2391, May 2019, doi: 10.1109/TIA.2019.2895797.

[2] B. Gou, Y. Xu, Y. Xia, G. Wilson, and S. Liu, "An intelligent time-adaptive data-driven method for sensor fault diagnosis in induction motor drive system," *IEEE Trans. Ind. Electron.*, vol. 66, no. 12, pp. 9817–9827, Dec. 2019, doi: 10.1109/TIE.2018.2880719.

[3] R. A. Lizarraga-Morales, C. Rodriguez-Donate, E. Cabal-Yepez, M. Lopez-Ramirez, L. M. Ledesma-Carrillo, and E. R. Ferrucho-Alvarez, "Novel FPGA-based methodology for early broken rotor bar detection and classification through homogeneity estimation," *IEEE Trans. Instrum. Meas.*, vol. 66, no. 7, pp. 1760–1769, Jul. 2017, doi: 10.1109/TIM.2017.2664520.

[4] S.-K. Kim and J.-K. Seok, "High-frequency signal injection-based rotor bar fault detection of inverter-fed induction motors with closed rotor slots," *IEEE Trans. Ind. Appl.*, vol. 47, no. 4, pp. 1624–1631, Jul. 2011, doi: 10.1109/TIA.2011.2153171.

[5] B. Luo, H. Wang, H. Liu, B. Li, and F. Peng, "Early fault detection of machine tools based on deep learning and dynamic identification," *IEEE Trans. Ind. Electron.*, vol. 66, no. 1, pp. 509–518, Jan. 2019, doi: 10.1109/TIE.2018.2807414.

[6] D. Reljic, D. Jerkan, D. Marcetic, and D. Oros, "Broken bar fault detection in IM operating under no-load condition," *Adv. Electr. Comput. Eng.*, vol. 16, no. 4, pp. 63–70, 2016, doi: 10.4316/AECE.2016.04010.

[7] T. Yang, H. Pen, Z. Wang, and C. S. Chang, "Feature knowledge based fault detection of induction motors through the analysis of stator current data," *IEEE Trans. Instrum. Meas.*, vol. 65, no. 3, pp. 549–558, Mar. 2016, doi: 10.1109/TIM.2015.2498978.

[8] G. H. Bazan, P. R. Scalassara, W. Endo, A. Goedtel, W. F. Godoy, and R. H. C. Palácios, "Stator fault analysis of three-phase induction motors using information measures and artificial neural networks," *Electr. Power Syst. Res.*, vol. 143, pp. 347–356, Feb. 2017, doi: 10.1016/j.epsr.2016.09.031.

[9] S. Zhang, C. Zhao, and F. Gao, "Incipient fault detection for multiphase batch processes with limited batches," *IEEE Trans. Control Syst. Technol.*, vol. 27, no. 1, pp. 103–117, Jan. 2019, doi: 10.1109/TCST.2017.2755580.

[10] A. Abid, M. T. Khan, H. Lang, and C. W. de Silva, "Adaptive system identification and severity index-based fault diagnosis in motors," *IEEE/ASME Trans. Mechatronics*, vol. 24, no. 4, pp. 1628–1639, Aug. 2019, doi: 10.1109/TMECH.2019.2917749.

[11] A. L. Martinez-Herrera, L. M. Ledesma-Carrillo, M. Lopez-Ramirez, S. Salazar-Colores, E. Cabal-Yepez, and A. Garcia-Perez, "Gabor and the wigner-ville transforms for broken rotor bars detection in induction motors," in *Proc. Int. Conf. Electron., Commun. Comput. (CONIELECOMP)*, Feb. 2014, pp. 83–87, doi: 10.1109/CONIELECOMP.2014.6808572.

[12] W. Liu, W. Chen, and Z. Zhang, "A novel fault diagnosis approach for rolling bearing based on high-order synchrosqueezing transform and detrended fluctuation analysis," *IEEE Access*, vol. 8, pp. 12533–12541, 2020, doi: 10.1109/ACCESS.2020.2965744.

[13] B. Pang, G. Tang, and T. Tian, "Complex singular spectrum decomposition and its application to rotating machinery fault diagnosis," *IEEE Access*, vol. 7, pp. 143921–143934, 2019, doi: 10.1109/ACCESS.2019.2945369.

[14] P. A. Panagiotou, I. Arvanitakis, N. Lophitis, J. A. Antonino-Daviu, and K. N. Gyftakis, "FEM approach for diagnosis of induction machines' non-adjacent broken rotor bars by short-time Fourier transform spectrogram," *J. Eng.*, vol. 2019, no. 17, pp. 4566–4570, Jun. 2019, doi: 10.1049/joe.2018.8240.

[15] A. Sapena-Bano, M. Riera-Guasp, R. Puche-Panadero, J. Martinez-Roman, J. Perez-Cruz, and M. Pineda-Sanchez, "Harmonic order tracking analysis: A speed-sensorless method for condition monitoring of wound rotor induction generators," *IEEE Trans. Ind. Appl.*, vol. 52, no. 6, pp. 4719–4729, Nov. 2016, doi: 10.1109/TIA.2016.2597134.

[16] A. Głowacz and Z. Głowacz, "Recognition of rotor damages in a DC motor using acoustic signals," *Bull. Polish Acad. Sci. Tech. Sci.*, vol. 65, no. 2, pp. 187–194, Apr. 2017, doi: 10.1515/bpasts-2017-0023.

[17] A. Glowacz and W. Glowacz, "Vibration-based fault diagnosis of commutator motor," *Shock Vibrat.*, vol. 2018, pp. 1–10, Oct. 2018, doi: 10.1155/2018/7460419.

[18] Y. Trachi, E. Elbouchikhi, V. Choqueuse, and M. E. H. Benbouzid, "Induction machines fault detection based on subspace spectral estimation," *IEEE Trans. Ind. Electron.*, vol. 63, no. 9, pp. 5641–5651, Sep. 2016, doi: 10.1109/TIE.2016.2570741.

[19] Y. Liu and A. M. Bazzi, "A review and comparison of fault detection and diagnosis methods for squirrel-cage induction motors: State of the art," *ISA Trans.*, vol. 70, pp. 400–409, Sep. 2017, doi: 10.1016/j.isatra.2017.06.001.

[20] J. R. Rivera-Guillen, J. J. De Santiago-Perez, J. P. Amezquita-Sanchez, M. Valtierra-Rodriguez, and R. J. Romero-Troncoso, "Enhanced FFT-based method for incipient broken rotor bar detection in induction motors during the startup transient," *Measurement*, vol. 124, pp. 277–285, Aug. 2018, doi: 10.1016/j.measurement.2018.04.039.

[21] P. A. Panagiotou, I. Arvanitakis, N. Lophitis, J. A. Antonino-Daviu, and K. N. Gyftakis, "A new approach for broken rotor bar detection in induction motors using frequency extraction in stray flux signals," *IEEE Trans. Ind. Appl.*, vol. 55, no. 4, pp. 3501–3511, Jul. 2019, doi: 10.1109/TIA.2019.2905803.

[22] A. Naha, A. K. Samanta, A. Routray, and A. K. Deb, "A method for detecting half-broken rotor bar in lightly loaded induction motors using current," *IEEE Trans. Instrum. Meas.*, vol. 65, no. 7, pp. 1614–1625, Jul. 2016, doi: 10.1109/TIM.2016.2540941.

[23] I. Ouachtouk, S. E. Hani, S, Guedira, K. Dahi, "Detection and classification of broken rotor bars faults in induction machine using K-means classifier," in *Proc. Int. Conf. Electr. Inf. Technol. (ICEIT)*, Tangiers, Morocco, May 2016, pp. 1–6, doi: 10.1109/EITech.2016.7519586.

[24] J. Burriel-Valencia, R. Puche-Panadero, J. Martinez-Roman, A. Sapena-Bano, and M. Pineda-Sanchez, "Cost-effective reduced envelope of the stator current via synchronous sampling for the diagnosis of rotor asymmetries in induction machines working at very low slip," *Sensors*, vol. 19, no. 16, pp. 1–16, Aug. 2019, doi: 10.3390/s19163471.

[25] D. G. Jerkan, D. D. Reljic, and D. P. Marcetic, "Broken rotor bar fault detection of IM based on the counter-current braking method," *IEEE Trans. Energy Convers.*, vol. 32, no. 4, pp. 1356–1366, Dec. 2017, doi: 10.1109/TEC.2017.2696578.

[26] L. A. Trujillo-Guajardo, J. Rodriguez-Maldonado, M. A. Moonem, and M. A. Platas-Garza, "A multiresolution Taylor–Kalman approach for broken rotor bar detection in cage induction motors," *IEEE Trans. Instrum. Meas.*, vol. 67, no. 6, pp. 1317–1328, Jun. 2018, doi: 10.1109/TIM.2018.2795895.

[27] C. G. Dias and F. H. Pereira, "Broken rotor bars detection in induction motors running at very low slip using a hall effect sensor," *IEEE Sensors J.*, vol. 18, no. 11, pp. 4602–4613, Jun. 2018, doi: 10.1109/JSEN.2018.2827204.

[28] V. Fernandez-Cavero, D. Morinigo-Sotelo, O. Duque-Perez, and J. Pons-Llinares, "Fault detection in inverter-fed induction motors in transient regime: State of the art," in *Proc. IEEE 10th Int. Symp. Diag. Electr. Mach., Power Electron. Drives (SDEMPED)*, Sep. 2015, pp. 205–211, doi: 10.1109/DEMPED.2015.7303691.

[29] B. Boashash, "Time-frequency signal analysis and processing," in *EURASIP and Academic Press Series in Signal and Image Processing*, 2nd ed. Oxford, U.K.: Kidlington, 2016.

[30] S.-C. Pei and S.-G. Huang, "Adaptive STFT with chirp-modulated Gaussian window," in *Proc. IEEE Int. Conf. Acoust., Speech Signal Process. (ICASSP)*, Apr. 2018, pp. 4354–4358, doi: 10.1109/ICASSP.2018.8462397.

[31] S. Kumar, R. Mehra, and Chandni, "Implementation and designing of FIR filters using kaiser window for de-noising of electrocardiogram signals on FPGA," in *Proc. IEEE 7th Power India Int. Conf. (PIICON)*, Nov. 2016, pp. 1–6, doi: 10.1109/POWERI.2016.8077428.

[32] M. Nilchian, J. P. Ward, C. Vonesch, and M. Unser, "Optimized kaiser–bessel window functions for computed tomography," *IEEE Trans. Image Process.*, vol. 24, no. 11, pp. 3826–3833, Nov. 2015, doi: 10.1109/TIP.2015.2451955.

[33] N. Otsu, "A threshold selection method from gray-level histograms," *IEEE Trans. Syst., Man, Cybern.*, vol. SMC-9, no. 1, pp. 62–66, Jan. 1979, doi: 10.1109/TSMC.1979.4310076.

[34] R. C. Gonzalez and R. E. Woods, *Digital Image Processing*, 4th. ed. London, U.K.: Pearson, 2018.

[35] M. Lopez-Ramirez, L. M. Ledesma-Carrillo, E. Cabal-Yepez, C. Rodriguez-Donate, H. Miranda-Vidales, and A. Garcia-Perez, "EMD-based feature extraction for power quality disturbance classification using moments," *Energies*, vol. 9, no. 7, pp. 1–15, Jul. 2016, doi: 10.3390/en9070565.

[36] Z. Wang, J. Yang, H. Li, D. Zhen, Y. Xu, and F. Gu, "Fault identification of broken rotor bars in induction motors using an improved cyclic modulation spectral analysis," *Energies*, vol. 12, no. 17, p. 3279, Sep. 2019, doi: 10.3390/en12173279.

[37] Y. Soleimani, S. M. A. Cruz, and F. Haghjoo, "Broken rotor bar detection in induction motors based on air-gap rotational magnetic field measurement," *IEEE Trans. Instrum. Meas.*, vol. 68, no. 8, pp. 2916–2925, Aug. 2019, doi: 10.1109/TIM.2018.2870265.

[38] W. Zhao and L. Wang, "Multiple-kernel MRVM with LBFO algorithm for fault diagnosis of broken rotor bar in induction motor," *IEEE Access*, vol. 7, pp. 182173–182184, 2019, doi: 10.1109/ACCESS.2019.2958689.
[39] S. B. Jiang, P. K. Wong, R. Guan, Y. Liang, and J. Li, "An efficient fault diagnostic method for three-phase induction motors based on incremental broad learning and non-negative matrix factorization," *IEEE Access*, vol. 7, pp. 17780–17790, 2019, doi: 10.1109/ACCESS.2019.2895909.
[40] J. L. Contreras-Hernandez, D. L. Almanza-Ojeda, S. Ledesma-Orozco, A. Garcia-Perez, R. J. Romero-Troncoso, and M. A. Ibarra-Manzano, "Quaternion signal analysis algorithm for induction motor fault detection," *IEEE Trans. Ind. Electron.*, vol. 66, no. 11, pp. 8843–8850, Nov. 2019, doi: 10.1109/TIE.2019.2891468.
[41] A. Glowacz, "Acoustic based fault diagnosis of three-phase induction motor," *Appl. Acoust.*, vol. 137, pp. 82–89, Aug. 2018, doi: 10.1016/j.apacoust.2018.03.010.

MISAEL LOPEZ-RAMIREZ (Member, IEEE) received the B.S. degree in electrical engineering and the M.E. and Ph.D. degrees from the University of Guanajuato, Guanajuato, Mexico, in 2011, 2013, and 2017, respectively. He concluded a Postdoctoral stay at the Technological Institute of Aguascalientes, Mexico. He joined the División de Ingenierías Campus Irapuato Salamanca, Universidad de Guanajuato, where he is currently a National Researcher with the Consejo Nacional de Ciencia y Tecnologia. His current research interests include image and signal processing, power quality, and digital systems applied to industry.

LUIS M. LEDESMA-CARRILLO (Member, IEEE) received the M.Eng. and Ph.D. degrees (Hons.) from the University of Guanajuato, Mexico, in 2013 and 2017, respectively. In 2017, he joined the División de Ingenierías Campus Irapuato Salamanca, Universidad de Guanajuato, where he is currently an Associate Professor. He is also a National Researcher with the Consejo Nacional de Ciencia y Tecnologia, Mexico. His research interests include digital signal and image processing on field-programmable gate arrays for applications in robotic vision and optics.

FRANCISCO M. GARCIA-GUEVARA received the bachelor's degree in electronics engineering from the Technological Institute of Aguascalientes, Mexico, in 2005, the M.Sc. degree in biomedical physic engineering from the Center for Research and Advanced Studies of the National Polytechnic Institute at Campus Monterrey (CINVESTAV), Mexico, in 2010, and the Ph.D. degree in engineering sciences from the Technological Institute of Aguascalientes, in 2017. He is currently doing a Postdoctoral stay at the University of Guanajuato at Yurira, His primary research interests include condition monitoring of electric machines, fault diagnosis, and signal processing.

JORGE MUNOZ-MINJARES received the B.S. degree in communications and electronic engineering from the Universidad Autonoma de Zacatecas, in 2010, and the M.S. degree in electrical engineering and the Ph.D. degree from the Universidad de Guanajuato (DICIS), in 2012 and 2018, respectively. His research interests include digital signal and image processing, optimal filtering, and probability and statistics.

EDUARDO CABAL-YEPEZ (Member, IEEE) received the M.Eng. degree from the Facultad de Ingenieria Mecanica Electrica y Electronica (FIMEE), Universidad de Guanajuato, Mexico, in 2001, and the Ph.D. degree from the University of Sussex, U.K., in 2007. In April 2008, he joined the División de Ingenierías Campus Irapuato Salamanca, Universidad de Guanajuato, where he is currently a Titular Professor. He is a National Researcher with the Consejo Nacional de Ciencia y Tecnologia, Mexico. He has authored more than 50 papers in international journals and conferences. His current research interests include digital image and signal processing, artificial intelligence, robotics, smart sensors, real-time processing, mechatronics, FPGA's, and embedded systems.

FRANCISCO J. VILLALOBOS-PINA (Member, IEEE) received the electronics engineering and the M.S. degree from the Aguascalientes Institute of Technology, Mexico, in 1998 and 2001, respectively, and the Ph.D. degree in electrical engineering from the Autonomous University of San Luis Potosí, in 2011. He is currently a Professor with the Electronics Engineering Department, Aguascalientes Institute of Technology. His research interests include power electronics, fault diagnosis, and control applied to electric machines.